

An accretion model for the eclipsing cataclysmic variable PG 0859+415

M. D. Still^{1,2}

¹*Physics and Astronomy, University of St. Andrews, North Haugh, St. Andrews, Fife KY16 9SS (mds1@st-and.ac.uk)*

²*Astronomy Centre, School of Mathematical and Physical Sciences, University of Sussex, Falmer, Brighton BN1 9QH*

Accepted 1996 May 20. Received 1996 April 25; in original form 1996 January 8

ABSTRACT

The emission lines found in the majority of cataclysmic variables are generally used as tracers of accretion flows which dominate the light at optical wavelengths. It has been suggested from previous observations that the eclipsing nova-like variable PG 0859+415 shows individualistic orbital characteristics which are inconsistent with canonical models of stellar accretion. We present spectrophotometry of this star which suggest that the standard picture is not in conflict with observation. We provide evidence that the shallow optical eclipses are of an extended bright spot rather than the accretion disc, and that the low-excitation lines are dominated by a transient absorption component, perhaps a result of the bright spot or accretion stream eclipsing the disc. We argue that this object may be another nova-like variable displaying long-term or cyclic variations in mass-transfer rate from the secondary star.

Key words:

accretion, accretion discs – binaries: eclipsing – binaries: spectroscopic – line: profiles – stars: mass-loss – stars: individual: PG 0859+415.

1 INTRODUCTION

PG 0859+415 is a 14th magnitude, eclipsing nova-like variable with an orbital period of 3.7 h (Grauer et al. 1994). As such, it is a member of the cataclysmic variable family, consisting of a red dwarf (the secondary star) transferring mass onto a white dwarf companion (the primary star) via Roche lobe overflow. Since there is no observational evidence for a significant magnetic field about the compact object, accretion is assumed to occur via a disc, which must be stable to variations in mass transfer rate in order to explain the lack of observed dwarf nova outbursts. A recent observational review of the nova-likes is provided by Dhillon (1996).

The majority of cataclysmic variables are emission line objects, which are used as tracers of the accretion flow that dominates the spectrum at optical wavelengths. In dwarf novae, emission features are superficially understood to be composites of lines from the accretion disc and the bright spot, where the gas stream from the secondary star impacts the outer rim of the disc (e.g. Marsh et al. 1990). Similar observations of the more energetic nova-likes, however, provide a complex picture which is proving difficult to unravel. Optical lines appear to be composites of both emission and absorption line spectra from a host of possible sources, such as the disc (Rutten et al. 1994), a disc wind (Honeycutt, Schlegel & Kaitchuck 1986), the bright spot (Still, Dhillon

& Jones 1995), the gas stream overflowing the accretion disc (Hellier & Robinson 1994), and the irradiated inner face of the secondary star (Beuermann & Thomas 1990). Given such a range of possible contributions to optical spectra, it is unsurprising that nova-like emission shows such diversity in properties and that the nova-like sub-classification scheme is constantly being questioned.

The blue excess object PG 0859+415 was confirmed as a cataclysmic variable during the optical campaign of Grauer et al. (1994; hereafter G94). Broad-band photometry showed rapid flickering and eclipses every 220 m, which was subsequently interpreted as the orbital period. Time-resolved spectroscopy reveals a high-excitation emission line spectrum with the higher Balmer series containing shallow absorption wings, presumably from the thick inner disc, and which display velocity modulation on the orbital period. The long-term constancy of light curves combined with the emission profiles suggest a nova-like classification.

Their data provided G94 with a number of provocative ideas. Firstly, photometry shows that eclipses are preceded by a broad hump, consistent with behaviour expected if the bright spot contributes to the optical flux. However, the depth of eclipse never exceeded the pre-hump photometric level – suggesting the possibility that the eclipse is of the bright spot, rather than the disc. Secondly, study of Balmer line profiles reveal a prominent narrow emission source with

Table 1. Journal of observations. E is the cycle number plus binary phase with respect to the ephemeris derived in Sec. 3.1.

Date (1995 Feb)	Start (UT)	End (UT)	Start (E - 12000)	End (E - 12000)	No. of spectra
16/17	23.66	3.90	326.43	327.58	46
17/18	22.77	3.94	332.73	334.14	40
18/19	22.84	3.98	339.29	340.69	35

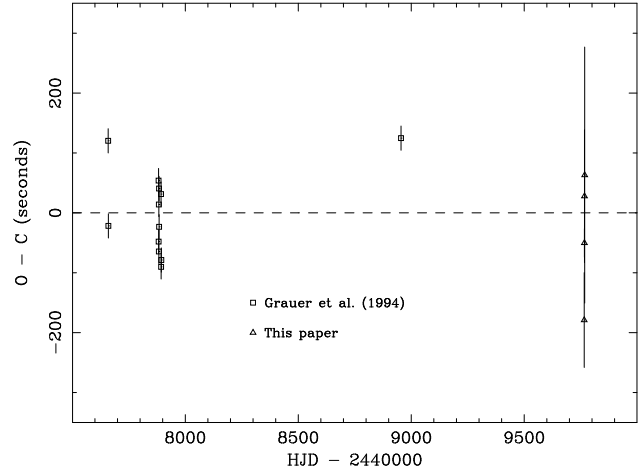
orbital-dependent velocities consistent with localized gas on the near side of the disc when observed at secondary star superior conjunction. Such a source is not predicted by models of disc accretion.

In this paper we present spectrophotometry of PG 0859+415, consistent with the data obtained by G94, and suggest an acceptable emission model which is a composite of secondary star irradiation, gas stream absorption and emission from a wind and/or an accretion disc. We find further evidence that the eclipsed source is the bright spot rather than the disc, providing an opportunity to study variations in mass transfer rate from the secondary star via changes in spot properties and disc size.

2 OBSERVATIONS

PG 0859+415 was observed on the nights beginning 1995 Feb 16-18 with the 2.5 m Isaac Newton Telescope on La Palma. Exposure times began at 140 s on Feb 16 but were increased over the night to optimize signal and orbital resolution. Dwell times of 400 s were decided upon and used for the rest of the run. Dead time for the dumping of data was generally 70 s between frames. The detector was a Tektronix CCD, windowed to 300×1124 pixels and mounted on the Intermediate Dispersion Spectrograph with a grating of 1200 lines mm^{-1} . This configuration gave a wavelength range of approximately $\lambda\lambda 5811\text{--}6671 \text{ \AA}$ at 1.7 \AA resolution. A journal of observations is given in Table 1. A nearby comparison star was placed on the slit and several photometric spectra were obtained through a wide slit for the purpose of flux corrections. CuAr arc exposures were taken every 30–40 m in order to calibrate the wavelength scale and instrumental flexure. The flux standard, Feige 66 (Massey et al. 1988), was observed with a wide slit to correct for instrumental response and convert the spectra to an absolute scale.

Medium-scale sensitivity variations were removed with a balance frame prepared from tungsten lamp and sky flat-fields. Fourth-order polynomial fits to the sky were subtracted and raw spectra were then extracted using the optimal algorithm of Horne (1986). Arc spectra for PG 0859+415, the comparison star and the flux standard were extracted from appropriate spatial locations on the arc frames. Fifth-order polynomial fits were made to the arc lines (rms scatter $< 0.05 \text{ \AA}$) and the wavelength scale for each spectrum was obtained by interpolating between two consecutive arc spectra. A comparison of the tabulated absolute flux values with a spline fit to the continuum of the flux standard provided a correction for large-scale instrumental response. Slit-loss corrections were achieved by dividing the PG 0859+415 spectra by a constant found from summing the flux under the continuum of the corresponding comparison star observation and multiplying by a constant derived

**Figure 1.** $O - C$ diagram for the times of mid-eclipse of PG 0859+415. The dashed line defines the linear ephemeris refined in this paper, the square symbols denote the photometric timings of G94 and the triangles are the spectrophotometric timings from the current data.**Table 2.** $O - C$ timings for mid-eclipses of PG 0859+415, relative to the new ephemeris.

Date (1995 Feb)	HJD	Cycle (E)	$O - C$ (s)
17	2 449 765.5760(9)	12 327	-179(79)
17	2 449 766.4943(3)	12 333	-50(24)
18	2 449 766.6481(13)	12 334	28(110)
19	2 449 767.5653(24)	12 340	63(213)

similarly from the average of the comparison star wide-slit exposures. A wavelength-dependent correction proved to be impossible due to the low photon counts in individual comparison star spectra.

3 RESULTS

3.1 Eclipse timings

Four eclipses were covered by these observations, providing an opportunity to test and refine the orbital ephemeris measured by G94. Eclipse profiles, which were produced by summing over line-free wavelengths of the continuum, were fitted with parabolae (details of light curve production may be found in Sec. 3.3). The minima of these, presented in Table 2, were combined with the photometric timings of G94 and fit with a linear function, giving an apparently improved orbital ephemeris of:

$$T_0 = \text{HJD } 2447881.8584(7) + 0.15281249(2) E$$

where T_0 is the time of mid-eclipse, and E is the subsequent orbital cycle number.

The residuals of this fit are presented in the $O - C$ diagram of Fig. 1. It is unclear whether the presence of outliers is systematic or statistical, but their significance is discussed in Sec. 4.

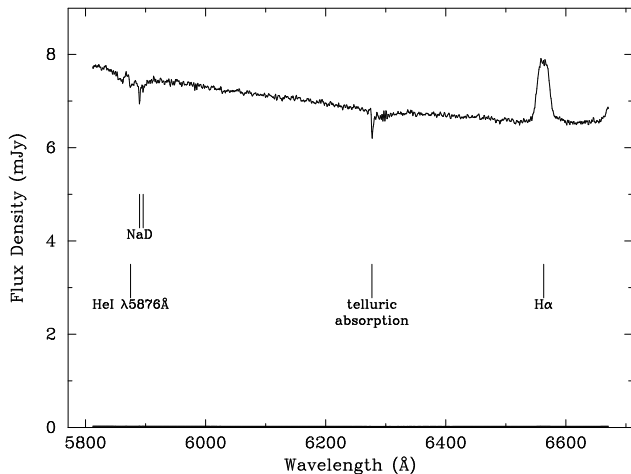


Figure 2. The average spectrum of PG 0859+415.

3.2 Average spectrum

The average of all spectra of PG 0859+415 is presented in Fig. 2. Given that the radial velocity of either stellar component remains unknown, spectra have not been re-binned to remove orbital line smearing. We find a strong blue continuum, superposed with weak emission lines of H α and He I λ 5876 Å. He I λ 5876 Å displays an emission core with shallow absorption wings and the red wing is blended with interstellar absorption. The strong continuum and He I profile suggest that a relatively large fraction of the disc is projected on the sky, compared to the deeply eclipsing members of the class (e.g. UX UMA: Rutten et al. 1994). The H α profile is single peaked, which is at odds with profiles of accretion disc emission, but this is not unexpected.

3.3 Spectrophotometry

A continuum light curve was produced by summing each exposure over the line-free wavelengths $\lambda\lambda$ 5929–6257 Å, $\lambda\lambda$ 6358–6506 Å and $\lambda\lambda$ 6625–6646 Å. This is presented in Fig. 3. Both the pre-eclipse hump and shallow eclipse are found in this light curve, although they appear less obvious than in the magnitude plots presented by G94 because of the linear scale, the range chosen to present the data, and nightly variations. Consistent with G94’s findings, the eclipse depth does not significantly exceed the pre-hump continuum level.

Line light curves were produced by subtracting a spline fit to the line-free continuum from the data, and summing over the profiles. There is no significant evidence for eclipse above the noise limits of either feature. The H α curve is similar to those of nova-likes whose lines are dominated by a component from the irradiated inner face of the secondary star (e.g. Dhillon, Jones & Marsh 1994). Given that stellar conjunction may not necessarily coincide with mid-eclipse (Sec 3.4), it is still true that maximum emission occurs at approximately the superior conjunction of the secondary star when, the inner, irradiated face of the star is most visible. The same behaviour may be found in the He I λ 5876 Å line, although the flux contribution is dominated by the absorption wings, most probably originating in the inner accretion disc.

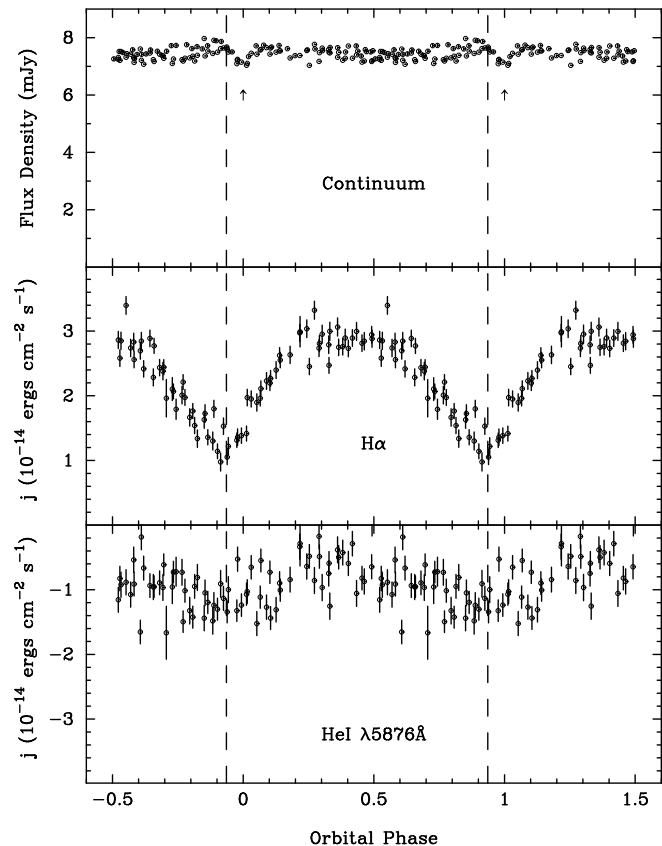


Figure 3. Orbital light curves for the continuum, H α and He I λ 5876 Å from PG 0859+415. Each curve is repeated over a second orbital cycle and orbital phase 0.0 corresponds to mid-eclipse and is marked by an arrow; however, the dashed lines, which are measured from Doppler images, are believed to be close to the true phase of stellar conjunction (Sec. 3.4).

If the secondary star is the major component of line emission, it will be evident in the orbitally-resolved line profiles. The data were averaged into phase bins, each covering 1/10 of the orbital cycle. Multiple offsets were applied to each and the resulting stack is plotted in Fig. 4. There appears to be at least two components to the H α line, suggesting that a line model containing only secondary star emission is inadequate. The profile consists of two anti-phased peaks, one consistent with an origin from the secondary star, and the other consequently associated with the primary star. This second peak is the feature identified by G94 as emission from a source at the front of the accretion disc, observed at superior conjunction of the secondary star. It should be noted however, that the profile can also be interpreted as one, or a composite of emission features, with a variable absorption component contaminating the core. Despite the small signal, the He I λ 4471 Å feature displays the same behaviour superposed over the broad absorption wings.

3.4 Line profile fitting

The data sampling and spectral resolution allow a more detailed analysis of the emission line profiles than the coarse phase bins of Fig. 4 allow. The data were continuum sub-

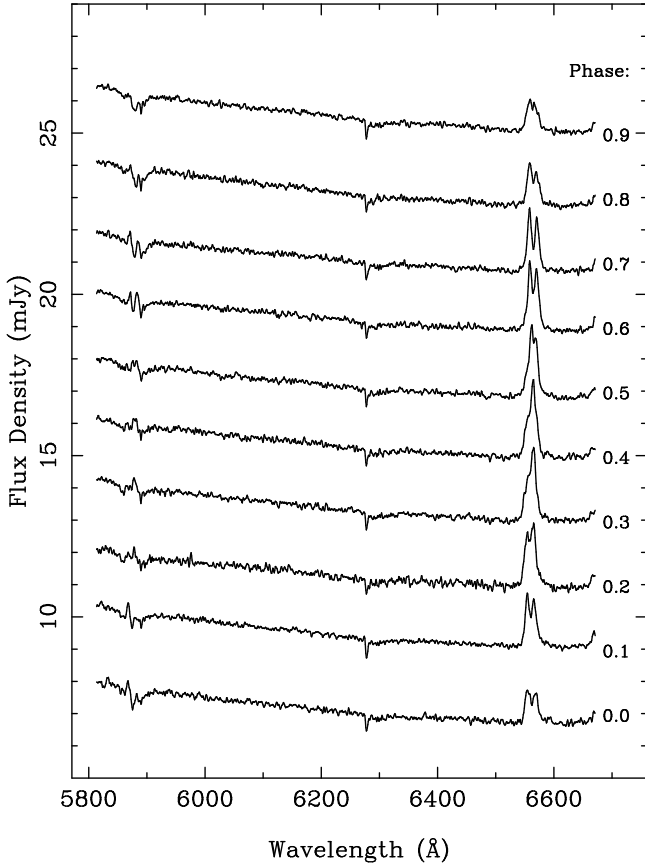


Figure 4. Orbital phase-binned spectra of PG 0859+415, stacked with offsets which are multiples of 4 mJy.

tracted in the usual way, re-binned onto a constant velocity scale of 39 km s^{-1} , and averaged into orbital phase bins each covering 2% of the orbit for $\text{H}\alpha$, and 5% for $\text{He I } \lambda 5876 \text{ \AA}$. The line profiles are presented as functions of orbital phase in Fig. 5. The linear grey-scale goes from white to black with increasing line intensity but has different zero points for each image, 0–3 mJy for $\text{H}\alpha$, and -0.6 – 0.1 mJy for $\text{He I } \lambda 5876 \text{ \AA}$. The data are repeated over a second orbital cycle and blank strips represent unfilled phase bins.

We first consider the $\text{H}\alpha$ feature, on which G94 base their analysis. The profile is dominated by two anti-phased emission components. The component with smaller velocity amplitude is approximately consistent with emission from the secondary star (Dhillon et al. 1994). Consequently, assuming a stellar mass ratio ($q = M_s/M_p$) less than unity, the anti-phased emission is consistent with a location on the back of the disc as viewed at the superior conjunction of the primary star, and as indicated by G94. Both emission components appear strongest at phase 0.5, as expected if the inferred spatial location of each source is correct. At orbital phases when the anti-phased emission does not dominate the profile, the line generally appears double-peaked, suggestive of a disc origin, or of absorption contamination from a local source within the accretion flow contaminating the core (Still et al. 1995).

Further insight into the line sources is often provided by image reconstruction using Doppler tomography (Marsh

& Horne 1988). This involves the mapping of velocity–phase data (V, ϕ) to a velocity–velocity field (V_x, V_y) via:

$$f(V, \phi) = \int_{-\infty}^{\infty} \int_{-\infty}^{\infty} I(V_x, V_y) \times g(V - \gamma + V_x \cos \phi - V_y \sin \phi) dV_x dV_y \quad (1)$$

where f is the line intensity at velocity V and orbital phase ϕ , I is the emission distribution of the resulting map in velocity coordinates (V_x, V_y), γ is the systemic velocity and $g(V)$ is the local line profile. Examples of similar image reconstructions may be found in e.g. Marsh & Horne (1990). Given that the profile of $\text{H}\alpha$ possibly contains an absorption component, the preferred method is that of Fourier-filtered back-projection (Horne 1992), thereby avoiding the positivity constraint demanded on reconstructions by a maximum entropy approach.

In order to reduce smoothing in the map, the data were convolved with a high-pass filter damped with a Gaussian cutoff to avoid high-frequency noise amplification. Back-projection results in the velocity map presented in Fig. 6. V_x is the abscissa and V_y the ordinate. Superposed over the image is an approximate binary configuration, where $K_s = 280 \text{ km s}^{-1}$ and $q = 0.5$. The secondary Roche lobe is plotted, with the trajectory of the accretion stream, originating at the inner Lagrangian point, and the Keplerian velocity about the white dwarf along the stream, originating from close to the secondary star’s centre of mass. This second trajectory represents the velocity of a Keplerian accretion disc at the spatial location of the stream (Marsh et al. 1990). The three crosses represent the centres of mass for the secondary star, binary and primary star. An orbital solution for PG 0859+415 is not known with any confidence and the choice of binary parameters is discussed shortly.

The features within this map are as expected from the trailed data. There are two major emission spots, one which we interpret as originating from the inner face of the the secondary star and the other, if we consider the velocity field to be that of a Keplerian accretion disc about the white dwarf, from a local source on the back of the accretion disc. A weaker ring is approximately centred on the primary star, suggestive of accretion disc emission. Fits to the line profiles, computed from the tomogram, are presented in Fig. 7. These are useful as a guide to the quality of the mapping procedure. Note, however, that pixel values in the map are not time-variable, and therefore the tomogram struggles to reconstruct the flux variations of individual line components within the data.

Clearly, the secondary star emission in the $\text{H}\alpha$ tomogram is not centred over the $V_x = 0$ axis. Provided we are willing to accept the secondary star as the origin for this feature, the most immediate explanation is that the eclipse ephemeris does not measure times of stellar conjunction. The consequent direction of coordinate rotation is consistent with the hypothesis of G94 that optical eclipses are of the bright spot only. A Gaussian fit to the secondary star peak indicates maximum emission at a velocity of $175 \pm 4 \text{ km s}^{-1}$, and 0.064 ± 0.002 orbital cycles before mid-eclipse. Since the secondary star emission is most likely to originate on its inner face, the measured velocity may be taken as a lower limit to the stars radial velocity semi-amplitude. The measured phase is an approximation of white dwarf superior

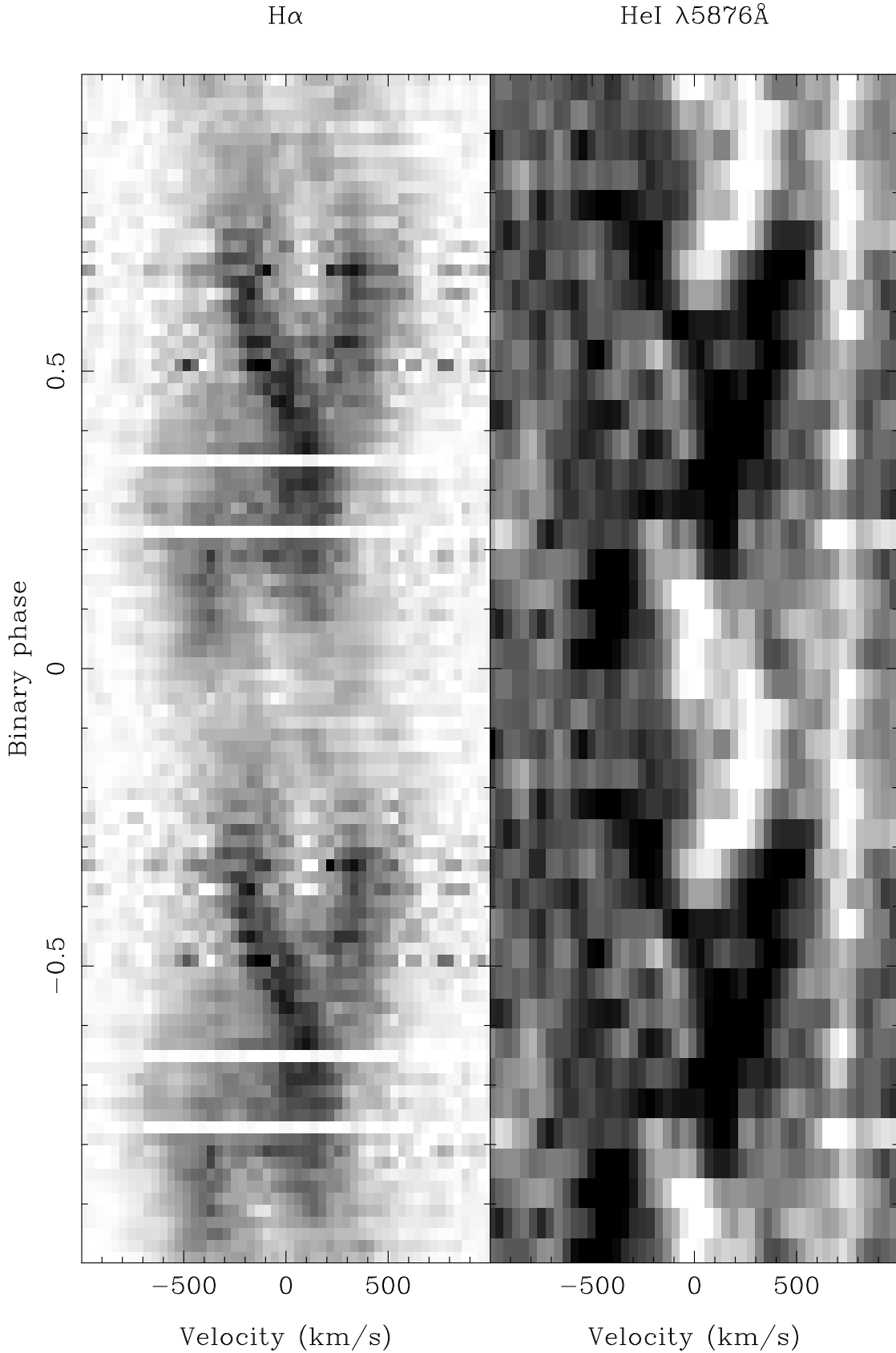


Figure 5. Trailed spectrograms of the $H\alpha$ and $He\text{I}\lambda 5876\text{ \AA}$ lines from PG 0859+415. The data has been repeated over a second orbital cycle and blank strips indicate unfilled phase bins. The two images are on separate linear intensity scales.

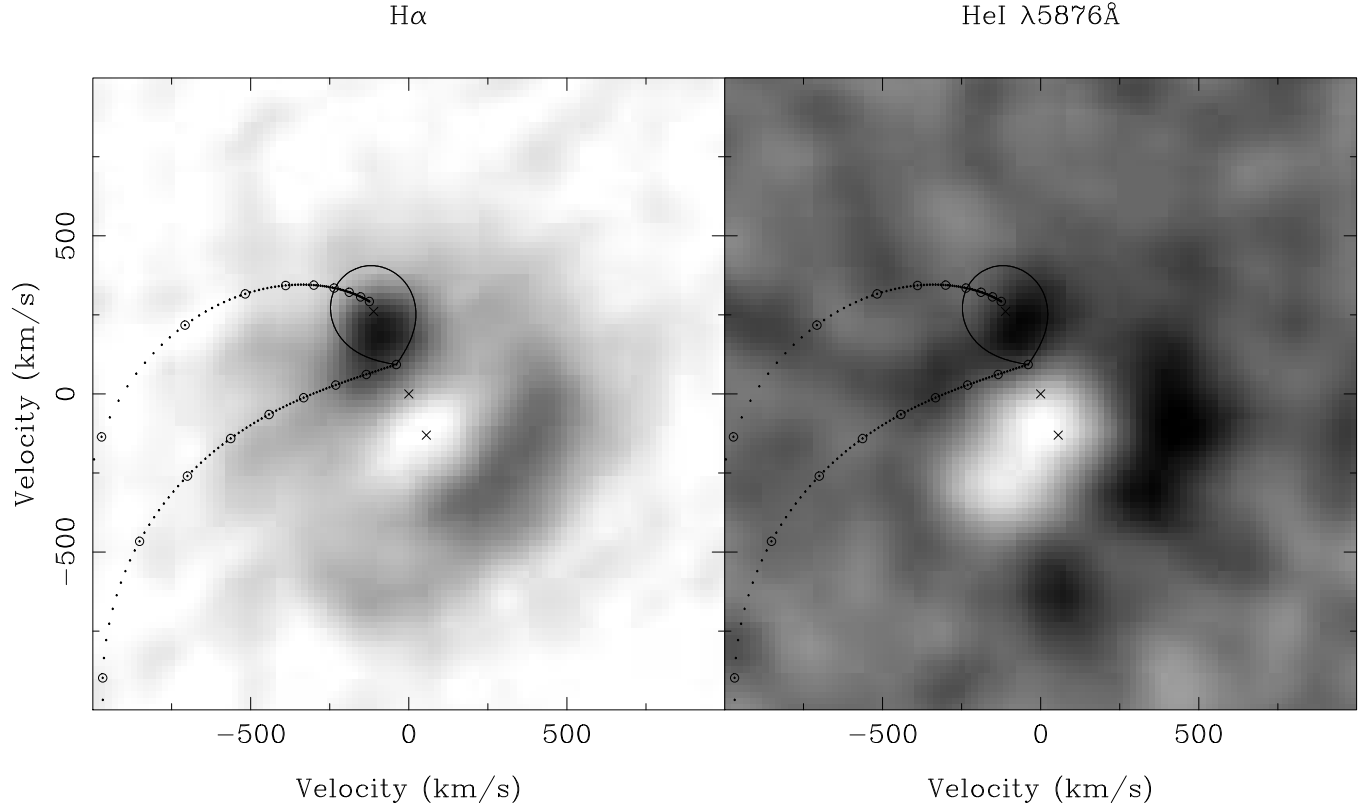


Figure 6. Doppler tomograms of the $H\alpha$ and $He\text{I}\lambda 5876\text{ \AA}$ feature from PG 0859+415. The intensity scales are linear but different for the two maps, where white to black illustrates increasing flux.

conjunction, which is illustrated by both the orientation of the binary on the tomograms and the dashed line found in Fig. 3. However, if irradiation of the secondary star is not symmetric about the L_1 -point, perhaps a consequence of shadowing by the bright spot or accretion stream (Southwell et al. 1995), then the conjunction phase will be inaccurate by no more than a few percent of the orbital period. The $H\alpha$ data are not suitable for providing a measurement of the primary star's radial velocity semi-amplitude since it remains unclear whether any of the emission is distributed symmetrically about the white dwarf (Shafter 1985; Still 1996). Therefore the binary parameters adopted for Fig. 6 are a guess, based on a mass ratio of $q = 0.5$ and assuming that only the inner face of the secondary star is irradiated.

The emission spot at the back of the disc has been inferred from two independent data sets, yet there appears no plausible reason for its presence. A solution is provided from an inspection of the $He\text{I}\lambda 5876\text{ \AA}$ profiles, which suggest that the spot is an artifact of core absorption. Fig. 5 illustrates that the two emission features found in the $H\alpha$ line are also observed in the $He\text{I}$ profile. Also present, however, is an absorption component which dominates the line core and has variable velocity and intensity over the orbital cycle, attaining maximum strength between orbital phases 0.6 and 1.1 and maximum velocity at phase 0.9. This provides a consistent, yet alternative, model for the line distribution: The first component is a broad emission feature which is visible in Fig. 5 between -500 km s^{-1} and $+500\text{ km s}^{-1}$; this is most likely from the accretion disc (Rutten et al. 1994),

or an accretion disc wind (Dhillon, Marsh & Jones 1991). The second is an absorption line overlaying the first component, similar to the feature observed in the deeply eclipsing nova-like RW Tri (Still et al. 1995), and the third is narrow emission from the secondary star (Dhillon et al. 1994). The last component appears to be faint but still visible at phase 0.9 where it is observed to cross the absorption feature. This is plausible given the inclination inferred by the shallow eclipse, and the superposition of this narrow component over the absorption provides confidence that it is an individual emission component and not the residue of core absorption.

With hindsight, this line model is equally plausible for the $H\alpha$ feature. The inferred spot at the back of the disc is a consequence of the same absorption component, found weakly in $H\alpha$, which depletes the broad emission component, leaving a residue which maps to the extended spot in Fig. 6.

Before back-projecting the suitably-filtered $He\text{I}\lambda 5876\text{ \AA}$ data, the interstellar features contaminating the red wing of the line were interpolated over. The resulting map, presented in Fig. 6, shows the features interpreted in the data as the secondary star component, the strong absorption core and the broad emission residual. Since the individual pixels within the map are time-independent, the narrow secondary star emission and the absorption core have not been reconstructed accurately. Hence, as is common, for nova-like emission, the computed profiles of Fig. 7 do not provide a good representation of flux variations in the data.

If incorporated into the model of Keplerian disc and

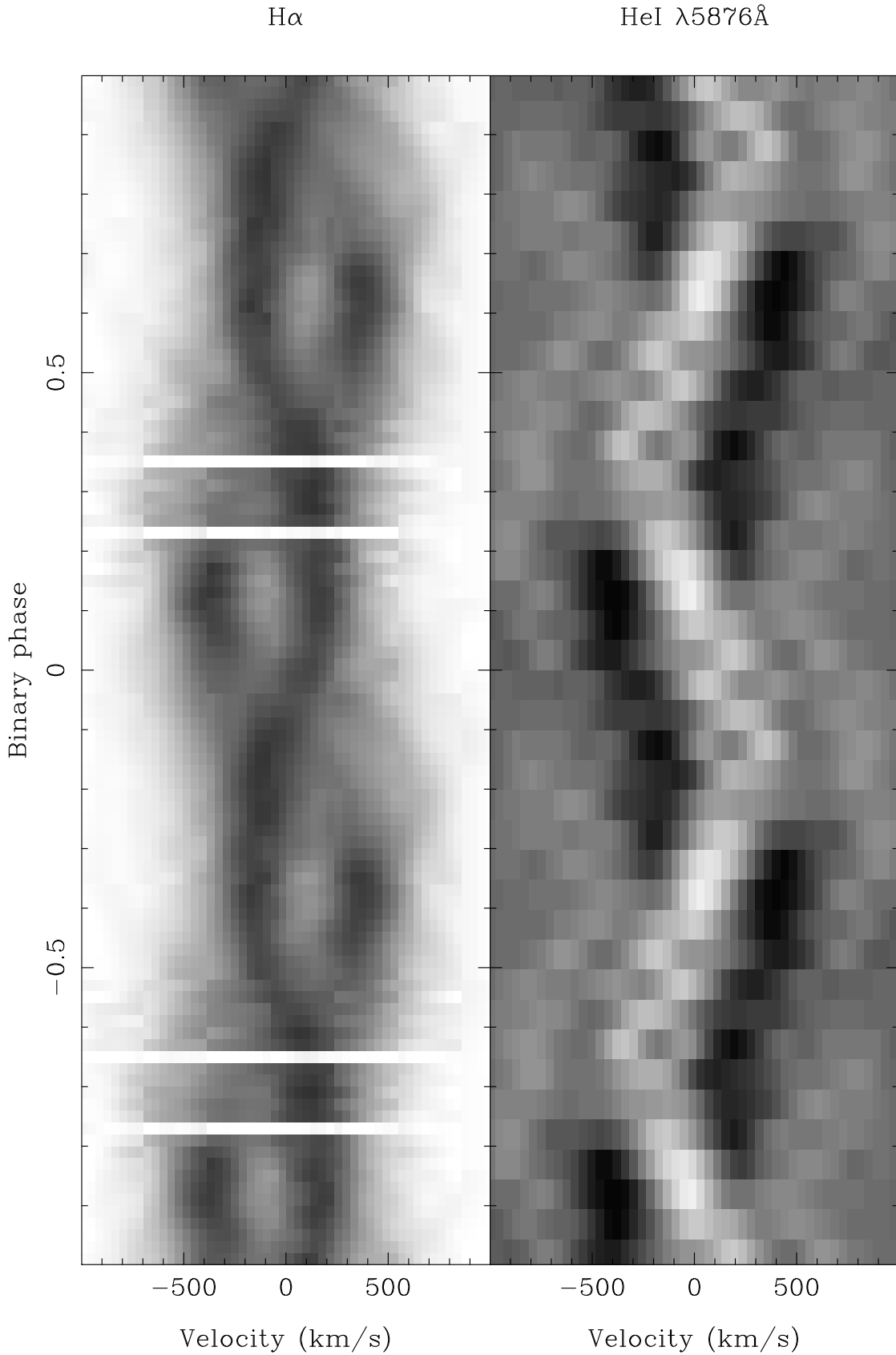


Figure 7. Model spectrograms of the $H\alpha$ and $He\ I\ \lambda 5876\ \text{\AA}$ lines from PG 0859+415, computed from the tomograms of Fig. 6. The data have been repeated over a second orbital cycle and blank strips indicate unfilled phase bins. The two images are on separate linear intensity scales.

ballistic accretion stream, both the map and computed profiles indicate that the absorption occurs on the trailing side of the disc, although it does not appear to coincide with either the gas stream trajectory or the Keplerian trajectory off the stream. Although there is some freedom to arrange the conjunction ephemeris and binary parameters according to the irradiation distribution on the inner face of the secondary star, there are no plausible configurations to allow the stream trajectories to coincide with the absorption velocities. However, absorption strength appears correlated with the continuum hump displayed by the optical continuum (G94 and Fig. 3), suggesting that the feature could be related to the bright spot or accretion stream. A possible interpretation of its velocity is that the disc is thicker downstream from the bright spot than upstream, and the disc rim at these azimuths is able to eclipse the inner disc – consistent with the model suggesting that it is the bright spot which is being eclipsed by the secondary star. The absence of absorption at the likely bright spot velocity is perhaps a consequence of core *filling* by emission from the spot or stream. The data is not of the desired quality to favour or refute this idea; more precise light curves of the lines features during eclipse are required for this purpose.

Certainly, the line distribution does not provide a unique emissivity model, however, the strength of the above interpretation is that it considers only accretion elements that are well-founded in both theory and observation.

4 DISCUSSION

The present data can be described by a model where the bright spot is the major contributor driving orbital phenomena in the nova-like variable PG 0859+415. The bright spot appears to be eclipsed by the secondary star, and low-excitation lines are dominated by a variable component, perhaps from the spot region, which occults the inner disc and provides a confusing set of emission profiles to deconvolve. Fig. 1 illustrates that there are a number of outlying eclipse times from the best linear orbital ephemeris. It is not implausible that these outliers are the result of misleading statistics. However, it may be that this distribution is not best fit by a linear ephemeris and is a result of variable mass transfer from the secondary star (Robinson, Shetrone & Africano 1991; Applegate 1992). If the emission model suggested by this data proves to be accurate, long-term photometric and spectroscopic monitoring of bright spot intensities and relative disc sizes, provided by eclipse times, may provide an opportunity to study the accretion flows response to variations in mass transfer rate from the secondary star. Further eclipse times are required to improve the statistics of the $O - C$ diagram before the significance of the linear ephemeris may be suitably tested.

5 CONCLUSIONS

The UX UMa nova-like classification made by G94 is consistent with the observation made in this paper that PG 0859+415 is a lower inclination analogue of UX UMa (Kaitchuck, Honeycutt & Schlegel 1983) and RW Tri (Still et al. 1995). Lines are interpreted as composites of the bright

spot and inner accretion disc in absorption, and the irradiated inner face of the secondary star and outer disc, or a disc wind, in emission. If unrecognised, the bright spot component, provides a confusing emission distribution which is at odds with models of disc accretion. Provided the identification of secondary star emission is correct, a lower limit to the radial velocity of the donor star is 280 km s^{-1} , and the eclipse found in the optical continuum must be dominated by the bright spot rather than the disc. Further eclipse times are required to determine the significance of outliers from the best linear orbital ephemeris, which may be indicative of variable mass transfer from the secondary star.

Acknowledgments

We thank Tom Marsh for the use and support of his spectral reduction packages PAMELA, MOLLY and DOPPLER, and Keith Horne and Paul Bennie for comments and suggestions. The Isaac Newton Group of telescopes are operated on the island of La Palma by the Royal Greenwich Observatory in the Spanish Observatorio del Roque de los Muchachos of the Instituto de Astrofísica de Canarias.

REFERENCES

- Applegate, J. H., 1992, *ApJ*, 385, 621.
 Beuermann, K., Thomas, H. C., 1990, *A A*, 230, 326.
 Dhillon, V. S., Marsh, T. R., Jones, D. H. P., 1991, *MNRAS*, 252, 342.
 Dhillon, V. S., Jones, D. H. P., Marsh, T. R., 1994, *MNRAS*, 266, 859.
 Dhillon, V. S., 1996, in *IAU symposium 158, Cataclysmic Variables and related Objects*, eds. Wood, J. H., Evans, A., in press.
 Grauer, A. D., Ringwald, F. A., Wegner, G., Liebert, J., Schmidt, G. D., Green, R. F., 1994, *AJ*, 108, 214 (G94).
 Hellier, C., Robinson, E. L., 1994, *ApJ*, 431, L107.
 Honeycutt, R. K., Schlegel, E. M., Kaitchuck, R. H., 1986, *ApJ*, 302, 388.
 Horne, K., 1986, *PASP*, 98, 609.
 Horne, K., 1992, in *Fundamental Properties of Cataclysmic Variable Stars*, 12th North American Workshop on Cataclysmic Variables and Low Mass X-ray Binaries, ed. A. Shafter, San Diego State University Press.
 Kaitchuck, R. H., Honeycutt, R. K., Schlegel, E. M., 1983, *ApJ*, 267, 239.
 Marsh, T. R., Horne, K., 1988, *MNRAS*, 235, 269.
 Marsh, T. R., Horne, K., 1990, *ApJ*, 349, 593.
 Massey, P., Strobel, K., Barnes, J. V., Anderson, E., 1988, *ApJ*, 328, 315.
 Robinson, E. L., Shetrone, M. D., Africano, J. L., 1991, *AJ*, 102, 1176.
 Rutten, R. G. M., Dhillon, V. S., Horne, K., Kuulkers, E., 1994, *A&A*, 283, 441.
 Shafter, A. W., 1985, in *Cataclysmic Variables and Low Mass X-ray Binaries*, eds. Lamb, D. Q., Patterson, J., Reidel, p. 355.
 Southwell, K. A., Still, M. D., Smith, R. C., Martin, J. S., 1995, *A&A*, 302, 90.33
 Still, M. D., Dhillon, V. S., Jones, D. H. P., 1995, *MNRAS*, 273, 849.
 Still, M. D., 1996, in *IAU symposium 158, Cataclysmic Variables and related Objects*, eds. Wood, J. H., Evans, A., in press.

This paper has been produced using the Royal Astronomical Society/Blackwell Science L^AT_EX style file.